Dynamic Order-Disorder in Atomistic Models of Structural Glass Formers

Lester O. Hedges[1,*], Robert L. Jack[1,2,*], Juan P. Garrahan[3], and David Chandler[1]

[1]*Department of Chemistry, University of California, Berkeley, California 94720-1460, USA.*
[2]*Department of Physics, University of Bath, Bath BA2 7AY, UK.*
[3]*School of Physics and Astronomy, University of Nottingham, Nottingham NG7 2RD, UK.*
[*]*These authors contributed equally to this work.*

Abstract

"The glass transition is the freezing of a liquid into a solid state without evident structural order. While glassy materials are well characterized experimentally, the existence of a phase transition into the glass state remains controversial. Here, we present numerical evidence for the existence of a novel first-order dynamical phase transition in atomistic models of structural glass formers. In contrast to equilibrium phase transitions, which occur in configuration space, this transition occurs in trajectory space, and it is controlled by variables that drive the system out of equilibrium. Coexistence is established between an ergodic phase with finite relaxation time and a non-ergodic phase of immobile molecular configurations. Thus, we connect the glass transition to a true phase transition, offering the possibility of a unified picture of glassy phenomena.

When super-cooled far below their melting temperatures, many liquids become extremely viscous, so much so that at low enough temperatures these materials become amorphous solids[1,2]. This phenomenon is termed the “glass transition”. The dynamical behavior of molecules in a glass is heterogeneous, in that there are domains of mobile and immobile molecules segregated in space[3-6]. At equilibrium, the spatial extent of these domains is large compared to molecular dimensions[5], but not so large to imply an actual phase transition. Indeed, and despite the name given to it, there is no observation

that demonstrates a link between the glass transition and a phase transition controlled by traditional thermodynamic variables like temperature and pressure.

Nevertheless, for idealized lattice models, recent work has established the existence of a non-traditional phase transition, one controlled by variables that drive a system out of equilibrium[7-9]. Here, we present numerical evidence for the same behavior in atomistic models of structural glass formers. We do so with a suitable form of transition path sampling[10] that allows us to study ensembles of long trajectories for supercooled fluids with several-hundred particles driven out of equilibrium by a field that couples to their mobility. By adjusting field strength, trajectories of these super-cooled fluids can be moved reversibly between ergodic and non-ergodic behaviors. The former are mobile states with finite relaxation times--the system forgets its initial state. The latter are immobile states that remember initial conditions for all time. At intermediate field strengths, trajectory space is filled by two coexisting domains, one that is ergodic and one that is non-ergodic.

In this way, it appears that dynamic heterogeneity observed in the equilibrium dynamics of super-cooled fluids is a precursor to a first-order phase transition in space-time. First-order transitions are associated with a discontinuity in an order parameter and a corresponding singularity in a partition function, such as the discontinuity in density for a liquid-vapor transition. These mathematical features emerge from the principles of statistical mechanics in the limit of a very large system, what is usually called the "thermodynamic" limit[11]. For finite systems studied numerically, there are no such singularities. Evidence of a phase transition in these cases is found in the behaviours of crossovers from one phase to another[12]. Figure 1 illustrates the system-size behaviour of a crossover. For the transition we consider, the partition function is a sum over dynamical histories (i.e., trajectories) of the system, and the order parameter measures the amount of activity or mobility that occurs among N particles in a volume V with trajectories that run for an observation time t_{obs}. As such, the pertinent measure of system size is a volume in space-time, the product $N \times t_{\text{obs}}$ or equivalently $V \times t_{\text{obs}}$. In the work reported here, we have considered spatial volumes that are 10 to 30 times larger than the correlation volume of the equilibrium system, and observation times that

are 10 to 100 times longer than a structural relaxation time of the un-driven system. These sizes are sufficient to exhibit behaviors suggestive of a non-equilibrium phase transition.

Equilibrium and Non-Equilibrium Phase Transitions

To discuss how these behaviors are revealed, let us first recall how Gibbs' statistical mechanics is used to study traditional equilibrium phase transitions[11]. Taking a system of N particles at a pressure p, we use the volume V as an order parameter, and take microstates to be points in configuration space, $x = (\mathbf{r}_1, \mathbf{r}_2, \ldots, \mathbf{r}_N)$, where the vector $\mathbf{r}_i$ denotes the position of the ith particle. Different phases, such as liquid and vapor, are distinguished from the other by the typical size of V. Changes in V are coupled to the thermodynamic field p or βp, where $1/\beta$ stands for Boltzmann's constant times temperature, $k_B T$. In particular, the probability of a configuration, x, is proportional to $P_0(x)\exp[-\beta \Delta p V(x)]$, where $P_0(x)$ is the probability of x at the reference field or pressure $p_0 = p - \Delta p$. The mean volume of the system with this distribution is $\langle V \rangle_p \equiv V_p$, which is depicted schematically in Fig. 1. A first-order phase transition is manifested by a discontinuity at the pressure $p = p^*$. At this value of the pressure, two phases coexist with respective volumes per particle v_1 and v_2.

At coexistence, the distribution function for the order parameter is bimodal. The two peaks in the distribution coincide with the two equilibrium phases. There is a low probability to observe an intermediate value of V, between Nv_1 and Nv_2 in Fig. 1. This low probability decreases exponentially with the free energy cost to form an interface between the phases. The interfacial free energy grows as $N^{1-1/d}$ where d is the dimensionality. In the limit of a large system, therefore, volumes between Nv_1 and Nv_2 can be achieved only through a direct constraint on the volume. Further, at coexistence, the presence of two macroscopic states means that the mean square fluctuation in the volume grows as N^2. Because the response of the volume to a change in pressure is $-\partial V_p/\partial p = k_B T \left\langle (V - V_p)^2 \right\rangle_p$, these large fluctuations mean that the width of the crossover illustrated in Fig. 1 vanishes as $1/N$.

Analogous statements for trajectory space begin with a choice of order parameter, which we have taken to be

$$K\left[x(t)\right] = \Delta t \sum_{t=0}^{t_{\text{obs}}} \sum_{j=1}^{N} \left|\mathbf{r}_j\left(t+\Delta t\right) - \mathbf{r}_j\left(t\right)\right|^2 ,$$

where $\mathbf{r}_j(t)$ and $x(t)$ refer to particle position and point in configuration space, respectively, now as functions of time t. This chosen order parameter depends upon the system's path or history over the observation period, $0 \le t \le t_{\text{obs}}$. Square brackets are used to indicate that the order parameter is a function of configurations $x(t)$ over the entire period. The incremental time, Δt, is assigned a value for which a particle in a normal liquid would typically move a distance of the order of a molecular diameter. The sum over time is done incrementally, every Δt, thus giving a total of $t_{\text{obs}}/\Delta t$ points in time that contribute. When particles are mobile, as in a normal liquid, $K[x(t)]$ is typically large; when particles are immobile, as in a glass, $K[x(t)]$ is typically small. An order-disorder transition reflecting extensive changes in particle mobility is reflected in a discontinuous mean value of $K[x(t)]$.

The next step is to consider the probability distribution for trajectories when this order parameter is coupled to a field s.[13,14] This distribution is proportional to $P_0\left[x(t)\right]\exp\left(-s\,K\left[x(t)\right]\right)$, where $P_0\left[x(t)\right]$ is the equilibrium probability distribution, i.e., the distribution at $s = 0$. The equilibrium distribution is for trajectories that are causal, time-reversal symmetric, and preserve an equilibrium distribution of microstates. Its partition function is trivial because the distribution is normalized, i.e., $1 = \sum_{x(t)} P_0\left[x(t)\right]$, where the sum over $x(t)$ is a sum over all trajectories. In contrast, the perturbed distribution

$$P_s\left[x(t)\right] \propto P_0\left[x(t)\right]\exp\left(-s\,K\left[x(t)\right]\right)$$

has a non-trivial partition function, which for positive s decreases with increasing t_{obs}. For the space of trajectories governed by that distribution at positive s, this space is compressed with increasing t_{obs}, and for large enough s, configurations favored by that

distribution are ones that are visited by immobile or non-ergodic trajectories. $P_s[x(t)]$ is therefore a distribution for trajectories of a system driven out of equilibrium.

Laboratory procedures for forming glass are non-equilibrium processes that stabilize configurations from which equilibration is impossible. One example is the preparation of ultra stable glasses via vapour deposition[15]. We use the field s as a mathematical device to access these same configurations, configurations that would have negligible statistical weight in an un-driven equilibrium dynamics. We do not address how a particular experimental protocol stabilizes these non-ergodic configurations. We do, however, address whether the domain of these configurations is sufficiently large to produce a non-equilibrium phase transition.

Transition Path Sampling of the *s*-Ensemble

In ordinary molecular dynamics or Monte Carlo trajectories of model systems, trajectories obey detailed balance and are presumed to be ergodic. Their distribution, $P_0[x(t)]$, can be sampled by either running a single trajectory for a time $n \times t_{\text{obs}}$, or equivalently carrying out a random walk through trajectory space, sampling n independent trajectories each of duration t_{obs}. The latter procedure is a method of transition path sampling[10]. To sample $P_s[x(t)]$, we use transition path sampling, but now accepting or rejecting random walk steps so as to preserve the weight $P_0[x(t)]\exp(-sK[x(t)])$. We call the collection of trajectories harvested in this way the "s-ensemble". In this ensemble, for models with sufficiently correlated dynamics, the distribution function for the order parameter can be bimodal, as indicative of an order-disorder transition[7-9]. This behavior is illustrated schematically in Fig. 1 in a fashion that stresses its analogy with the corresponding behavior of an equilibrium phase transition.

In particular, the average value of the order parameter we have chosen is extensive in space-time, i.e., $K_s = \langle K[x(t)] \rangle_s$ is proportional to $N \times t_{\text{obs}}$, where the proportionality constant is the mean-square displacement of a particle in an incremental

time Δt. If two dynamical phases coexist – one with proportionality constant k_a, the other with k_i – then K_s will be a discontinuous function of s at the condition of coexistence, $s = s^*$. As illustrated with Fig. 1 for a finite system, the corresponding crossover will have width of the order of $1/Nt_{obs}$ because the mean square fluctuations in the order parameter grow as $(Nt_{obs})^2$. Further, the excess in free energy to maintain a coexisting ensemble grows as an interfacial area in space-time so that trajectories manifesting this coexistence are suppressed by a factor that depends exponentially on this area. In some cases[8], this area scales as $N^{1-1/d}t_{obs}$. The value s^* is proportional to the rate at which configurations from the non-ergodic "inactive" phase relax back to the ergodic equilibrium fluid if the driving field s is removed. In kinetically constrained lattice models[9], which are idealized models of structural glass formers[16], this rate is zero, i.e., $s^*=0$. In other words, for those models, un-driven equilibrium dynamics coexists with a non-ergodic phase. Here, we show that for more realistic atomistic models, and therefore for real glass forming materials, s^* is small although perhaps non-zero.

The particular system we have considered is Kob and Andersen's (KA) two-component mixture of Lennard-Jones particles[17]. It has $N_A = 0.8N$ principal particles, each with Lennard-Jones diameter σ and energy parameter ε. In addition, it has $N_B = 0.2N$ smaller secondary particles, where their size and attractive energy parameters are chosen so as to frustrate crystallization[17]. The structural and dynamical properties we report for this model, including the order parameter $K[x(t)]$, refer to the principal particles. We have carried out two independent studies, one where trajectories are governed by Newtonian molecular dynamics, and the other where trajectories are governed by a Monte Carlo dynamics. With appropriate scaling of time, both studies yield similar results. The results shown in the figures of this paper are from the molecular dynamics studies. For the incremental time, we use $\Delta t = 13.33\left(m\sigma^2 / 48\varepsilon\right)^{1/2}$, where m is the mass of the particles. Results from the Monte Carlo dynamics plus additional information about our computations are presented in Supplementary Information[18]. In terms of the reduced temperature $k_B T / \varepsilon$, the KA model behaves as an ordinary simple fluid at temperatures $k_B T / \varepsilon > 1$, but its relaxation

slows and large glassy fluctuations appear at lower temperatures. Around $k_B T / \varepsilon = 0.4$, relaxation becomes so slow that equilibration of the model on current-day computers becomes intractable. For what is shown below, we work at less severe but nonetheless non-trivial super-cooled conditions, $0.6 \le k_B T / \varepsilon \le 0.7$.

Although the system does not crystallize under equilibrium conditions, biasing the super-cooled KA model toward an inactive phase, as we do with transition path sampling of the *s*-ensemble, can induce crystallization. The effect is pronounced for small periodically replicated systems. It occurs because $K[x(t)]$ by itself does not discriminate between glass and crystal. Although one phase is an equilibrium phase and the other is not, both have low mobility. Thus, in addition to accounting for the value of K, our transition path sampling must also account for a measure of crystallinity. In particular, we use a common neighbour analysis[19], and bias against trajectories with this measure of crystallinity [see Supplementary Information[18]].

Bistability and Phase Transition in Trajectory Space

Our findings for the mean order parameter and its distribution in the *s*-ensemble (Fig. 2) reflect the qualitative features associated with a first-order phase transition. Tthe quantitative analysis of finite-size scaling is beyond the capabilities of the algorithms we have used in this work, but the results we have obtained are strikingly similar to those established in idealized kinetically constrained models of glass formers[7-9]. The susceptibility,

$$\chi_s = -\frac{\partial K_s}{\partial s} = \left\langle \left(K\left[x(t)\right] - K_s \right)^2 \right\rangle_s \quad ,$$

has a peak that grows with increasing N and t_{obs}. The peak position is the finite system estimate of s^*.[20] Its value decreases with increasing N and t_{obs} [system size scaling shown in Supplementary Information[18]]. The order parameter distribution is bimodal at this value of s, and the minimum between its two peaks decreases with increasing N and

t_{obs}. For the range of values of N and t_{obs}, the effects of increasing t_{obs} are greater than those of increasing N. This asymmetry in the dependence on N and t_{obs} is also reflected in the structure of space-time at coexistence. We will describe this structure, but first discuss a measure of ergodicity.

The particular measure we consider is the behavior of the function

$$F_s(q,t) = \frac{1}{Nt_{\text{obs}}} \sum_{t'=0}^{t_{\text{obs}}} \sum_{i=1}^{N} \left\langle \exp\left\{ i\mathbf{q}\bullet\left[\mathbf{r}_i(t+t') - \mathbf{r}_i(t')\right]\right\}\right\rangle_s .$$

At equilibrium, i.e., $s = 0$, $F_s(q,t)$ is the Van Hove self-correlation or intermediate-scattering function[21]. In general, it is a mean overlap between configurations displaced by a time t. The extent to which it is non-zero in the limit of large t is a measure of non-ergodicity[22]. We choose the wave vector q to coincide with the first maximum in the structure factor of the liquid (or glass). With this choice, the time τ for which $F_0(q,\tau) = 1/e$ is a common definition of the structural relaxation time. $F_s(q,t)$ is shown in Fig. 3 for the active (i.e., ergodic) and inactive (i.e., non-ergodic) phases. The relaxation time of the active trajectories is much less than t_{obs}, yet inactive trajectories remain trapped in a single state throughout the observation time. Figure 3 also shows the radial distribution function for the principal component of the mixture in the active and inactive states. This average measure of structure in the phase that can equilibrate ($s = 0$) is virtually identical to that for the phase that is driven to a non-ergodic state ($s > 0$). Thus, fluctuations from the mean structure are crucial to the difference between glassy materials and fluid materials.

Figure 4 illustrates the structure of trajectory space at conditions of active-inactive coexistence, i.e., at $s = s^*$. Each panel illustrates an overlap matrix, $Q(t,t') = N^{-1}\sum_{i=1}^{N} \cos\left\{\mathbf{q}\bullet\left[\mathbf{r}_i(t) - \mathbf{r}_i(t')\right]\right\}$, recording the similarity or overlap on a given trajectory between configurations at different times t and t'. The s-ensemble average of this quantity gives $F_s(q,t-t')$. The pictures in Fig. 4 illustrate the fluctuations from the mean, with the distance from the diagonal reflecting the time interval $t-t'$. At $s = s^*$, there are some trajectories with relatively high values of K indicative of the

active phase, others with relatively low values indicative of the inactive phase, and finally those that are intermediate and that demonstrate phase coexistence. Figure 4C shows a representative trajectory with a value of K corresponding to the active phase; see Fig. 2F. Here, motion is plentiful and the system quickly de-correlates as $t - t'$ grows.

In contrast, the overlap matrix for inactive trajectories, as illustrated in Fig. 4A, is homogeneous. The system remains correlated for the entire observation time, so that $Q(t,t')$ is large even when $|t-t'|$ is much greater than a structural relaxation time τ. Figure 4B shows a trajectory where the active and inactive phases are separated by a sharp temporal interface. These figures might seem to resemble those found for trajectories of small equilibrium sub-systems over time periods that are small compared to the structural relaxation time[23,24]. However, overlap matrices for trajectories of an equilibrated system reveal a structure in space-time in which the system undergoes multiple transitions between collections of states with low energy and activity, commonly termed "meta-basins". Typical lifetimes for these inactive basins are of the order of a fraction of τ. These lifetimes are negligible compared to the very long lifetimes of inactive states within the s-ensemble.

Figure 5 illustrates the correlations between the order parameter K and the behaviors of potential energy and icosahedral ordering at the coexistence field s^*. The potential energy of the inactive configurations is smaller, consistent with their stability. For active trajectories, particles sample many configurations, which leads to the self-averaging of structural measures and is reflected in the width of the distribution, which is significantly narrower for greater K. However, a clear correlation between potential energy and dynamics does not imply a causal link. Indeed, this thermodynamic variable cannot control the first-order transition we describe here. Rather, we must look to variables that measure dynamics over a period of time. Although there is a gradual increase in icosahedral ordering[19] as K decreases, the observed correlation is far weaker than that of the potential energy. The broad distribution at small K is once again indicative of fluctuation dominance within the inactive phase.

Fluctuations, Wetting and Critical Points

The existence of a first-order transition has many consequences. For example, fluctuations in an equilibrium system near to phase coexistence grow rapidly as the surface tension between these phases is reduced. Figure 2 indicates that the KA mixture is near a coexistence line between active and inactive phases, at both of the temperatures that we considered. Further, as the temperature is reduced, the values of K for the two phases approach each other, indicating that the surface tension between the phases will decrease as temperature decreases. We may therefore associate this decrease with the growth of fluctuations within the active phase. These fluctuations are the dynamical heterogeneities[5,6] in the equilibrium dynamics of the glass former. A further consequence of phase coexistence is the occurrence of wetting phenomena[25]. In the case of the dynamical transition discussed here, "wetting" is remembering the initial conditions, and an example of this behavior can be seen for $F_s(q,t)$ in Fig. 3B. At $s > s^*$ the initial time surface is fully wetted by the inactive phase. At $s = 0 < s^*$ there is only a film of finite thickness in time, precursor to the wetting transition.

For some idealized kinetically constrained models[7-9], coexistence between active and inactive phases along the s = 0 line ends at a T = 0 critical point. We expect similarly that for the KA mixture, the order parameters of both the active and inactive phases will approach the same value, $K_s \to 0$ as $T \to 0$ and s = 0. However, where active-inactive coexistence is present in the kinetically constrained models for all temperatures when s = 0, the same cannot be true for models with finite intermolecular forces. At high enough temperatures, such forces are insufficiently constraining to produce collective behavior. Indeed, we have found that at small values of s, the order parameter distribution for the KA mixture ceases to be bimodal when $k_B T/\varepsilon$ is significantly larger than 1 (see Supplementary Information[18]). One possibility is that the first-order coexistence line ends at an upper critical point at finite s and T. This possibilities remains to be investigated.

The first-order transition we have described is to be contrasted with the scenario that emerges from other approaches, such as mode-coupling theory[26,27] and the random first-order transition theory[28,29]. These theories predict the existence of dynamic or thermodynamic transitions controlled by thermodynamic fields such as temperature or

pressure. In contrast, our results show that the order-disorder transition is in the trajectories of the dynamics and is thus controlled by dynamic fields. Perhaps a thermodynamic manifestation can be related to the picture of an avoided phase transition[30]. In any case, our numerical results here suggest that in real glass formers this dynamical order-disorder phenomenon is close to that predicted from idealised kinetically constrained models[7-9]. Thus, we pass the baton to the experimenters to find protocols for controlling the dynamic observable K or driving field s that allow experimental probes of the transition described in this work.

1. M.D. Ediger, C.A. Angell, and S. Nagel, J. Phys. Chem. **100**, 13200 (1996).
2. P.G. Debenedetti and F.H. Stillinger, Nature **410**, 259 (2001).
3. K. Schmidt-Rohr and H. Spiess, Phys. Rev. Lett. **66**, 3020 (1991)
4. E. Weeks, J.C. Crocker, A.C. Levitt, A. Schofield, and D.A. Weitz, Science **287**, 627 (2000)
5. M.D. Ediger, Annu. Rev. Phys. Chem. **51**, 99 (2000).
6. S.C. Glotzer, J. Non-Cryst. Solids **274**, 342 (2000).
7. M. Merolle, J.P. Garrahan and D. Chandler, Proc. Natl. Acad. Sci. USA **102**, 10837 (2005).
8. R.L. Jack, J.P. Garrahan and D. Chandler, J. Chem. Phys. **125**, 184509 (2006).
9. J.P. Garrahan, R.L. Jack, V. Lecomte, E. Pitard, K. van Duijvendijk and F. van Wijland, Phys. Rev. Lett., **98** 195702 (2007).
10. P. G. Bolhuis, D. Chandler, C. Dellago, and P. L. Geissler, Annu. Rev. Phys. Chem. **53**, 291 (2002).
11. D. Chandler, "Introduction to Modern Statistical Mechanics" (OUP, Oxford, 1987).
12. D.P. Landau and K. Binder, "A Guide to Monte Carlo Simulations in Statistical Physics" (Cambridge University Press, Cambridge, 2000); see section 4.2.3.
13. J.-P. Eckmann and D. Ruelle, Rev. Mod. Phys. **57**, 617 (1985).

14. V. Lecomte, C. Appert-Rolland and F. van Wijland, J. Stat. Phys. **127**, 51 (2007).

15. S.F. Swallen, K.L. Kearns, M.K. Mapes, Y.S. Kim, R.J. McMahon, M.D. Ediger, T. Wu, L. Yu, S. Satija, Science **315**, 353 (2007).

16. F. Ritort and P. Sollich, Adv. Phys. **52**, 219 (2003).

17. W. Kob and H.C. Andersen, Phys. Rev. Lett. **73**, 1376 (1994).

18. Supporting materials are available for this article at *Science Online*.

19. J.D. Honeycutt and H.C. Andersen, J. Phys. Chem. **91**, 4950 (1987).

20. C. Borgs and R. Kotecky, Phys. Rev. Lett. **68**, 1738 (1992).

21. J.P Hansen and I.R. McDonald, "The Theory of Simple Liquids" (Academic Press, 2006).

22. S.F. Edwards and P.W. Anderson, J. Phys. F **5**, 965 (1975).

23. B. Doliwa and A. Heuer, Phys. Rev. E **67**, 031506 (2003).

24. G.A. Appignanesi, J.A. Rodríguez Fris, R.A. Montani, W. Kob, Phys. Rev. Lett. **96**, 57801 (2006).

25. H. Nakanishi and M.E. Fisher, Phys. Rev. Lett. **49**, 1565 (1982).

26. W. Gotze and L. Sjogren, Rep. Prog. Phys. **55**, 241 (1992).

27. D.R. Reichman and P. Charbonneau, J. Stat. Mech., P05013 (2005).

28. T.R. Kirkpatrick, D. Thirumalai and P. Wolynes, Phys. Rev. A **40**, 1045 (1987).

29. J.P. Bouchaud and G. Biroli, J. Chem. Phys. **121**, 7347 (2004).

30. D. Kivelson, S.A. Kivelson, X.L. Zhao, Z. Nussinov and G. Tarjus, Physica A **219**, 27 (1995).

31. During the course of this work we have benefited from discussions with Thomas F. Miller, III, and Frédéric van Wijland. The work was made possible through grants from the National Science Foundation (CHE-0543158 in the early stages fir RJ and DC, and CHE-0626305 in the later stages for LH and DC), from the US Office of Naval Research (N00014-07-1-0689 in the late stages for RJ), and from the EPSRC (GR/S54074/01 for JPG).

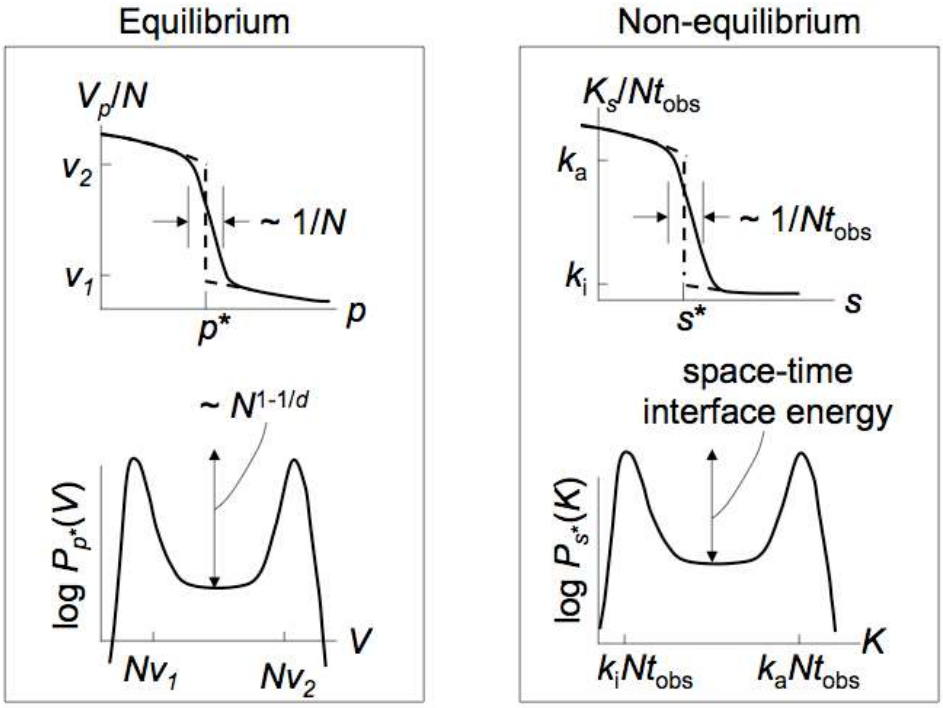

Fig. 1. Finite size effects of equilibrium and non-equilibrium phase transitions. The mean volume V_p manifests an equilibrium first-order phase transition at pressure $p = p^*$ while the mean dynamical activity K_s manifests a dynamical first-order phase transition at the dynamical field $s = s^*$. At conditions of phase coexistence, the volume distribution function, $P_p(V)$, and the dynamical activity distribution, $P_s(K)$, are bi-modal. Configurations or trajectories with intermediate behaviours lie at much higher free energies (or lower probabilities) than those of the basins. For finite systems, discontinuous phase transitions become crossovers with widths that vanish as system size, N, and observation time, t_{obs}, grow to infinity.

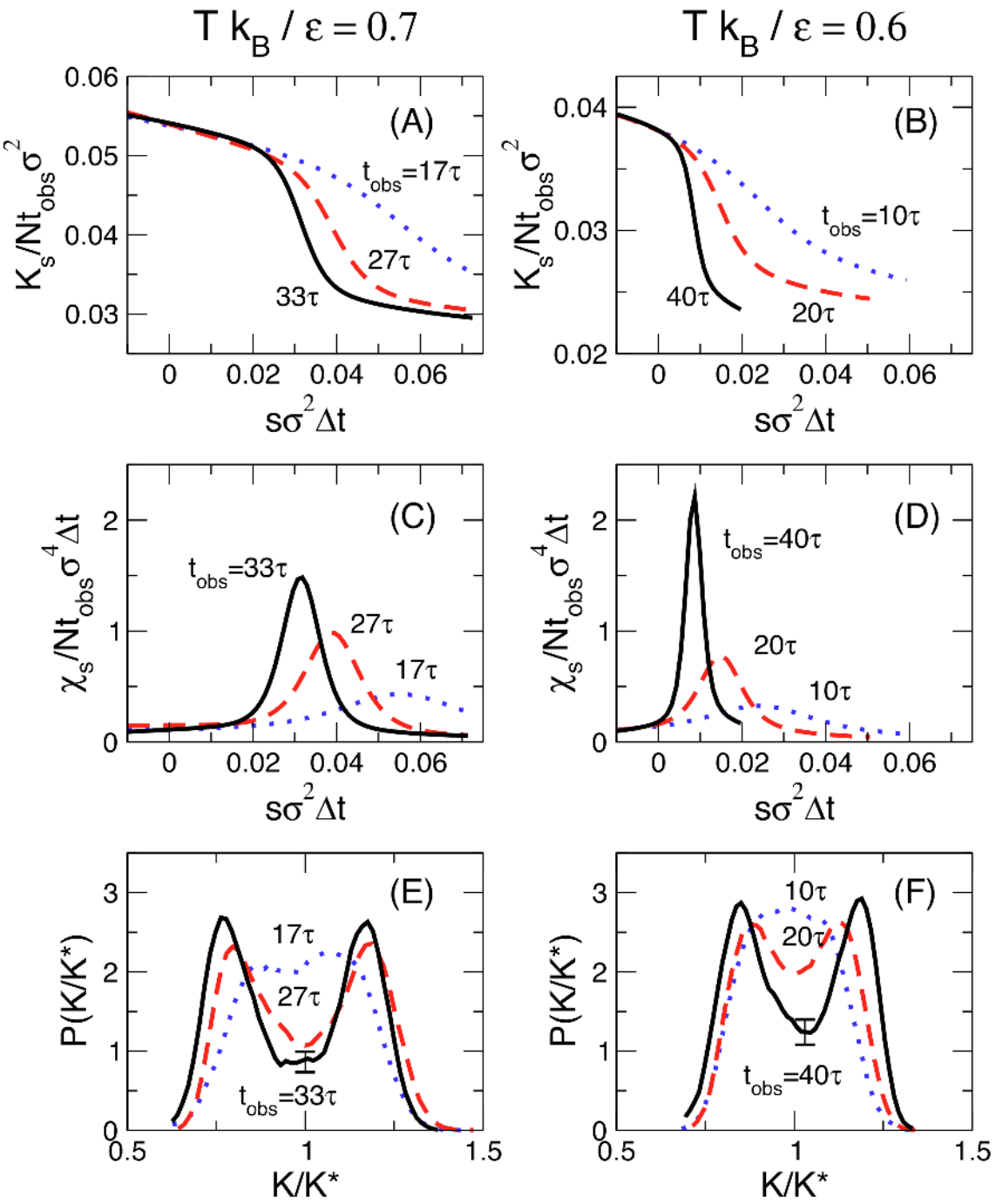

Fig. 2. Evidence for first-order phase transition in space-time. (A and B) Average space-time order parameter $K_s = \langle K[x(t)] \rangle_s$ as a function of field s, from molecular dynamics simulations of the Kob-Andersen Lennard-Jones mixture for $N = 150$ total

particles, at reduced temperatures $k_B T/\varepsilon = 0.6$ and $k_B T/\varepsilon = 0.7$, and principal component density $N_A \sigma^3 / V = 0.96$. ε and σ are the Lennard-Jones parameters for the larger (principal component) particles in the Kob-Andersen mixture. As the length of trajectories increases, the crossover in K_s becomes sharper and happens at smaller values of s. (C and D) The peak in the susceptibility $\chi_s = -\frac{\partial K_s}{\partial s}$ becomes larger and its position moves to smaller s with increasing t_{obs}. The crossover of K_s reflects a first-order transition in the infinite size limit. (E and F) Distribution of K at coexistence (where $K^* = K_s$ for $s = s^*$). For large t_{obs}, the order parameter distribution at the coexistence field s^* becomes bimodal, as expected for a first-order transition.

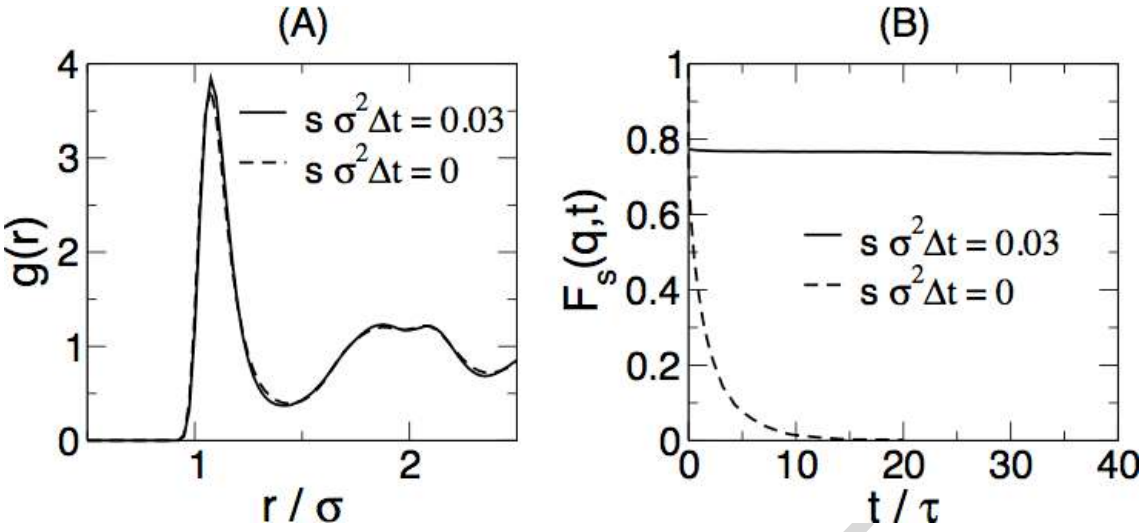

Fig. 3. Comparison of structure and dynamics of active and inactive phases. (A) Radial distribution function for the atoms of the principal component in the Kob-Andersen mixture. The equilibrium Kob-Andersen mixture is at $s = 0$. The non-equilibrium mixture is at $s = 0.03/\sigma^2 \Delta t > s^*$. Here, σ is the Lennard-Jones diameter for the principal component atoms, and $\Delta t = 13.33\left(m\sigma^2/48\varepsilon\right)^{1/2} \simeq \tau/15$, where τ is the structural relaxation time. There is no appreciable difference in the static structure of the active, $s < s^*$, and inactive, $s > s^*$, dynamical phases. (B) Self-intermediate scattering function for the same values of s. In the active phase correlation functions relax to zero. In the inactive phase correlation functions remains at a non-zero value even for the longest times; the inactive phase is non-ergodic. These results were obtained using simulations of $N = 150$ total particles, at reduced temperature and principal component density $k_B T/\varepsilon = 0.6$ and $N_A \sigma^3/V = 0.96$, respectively.

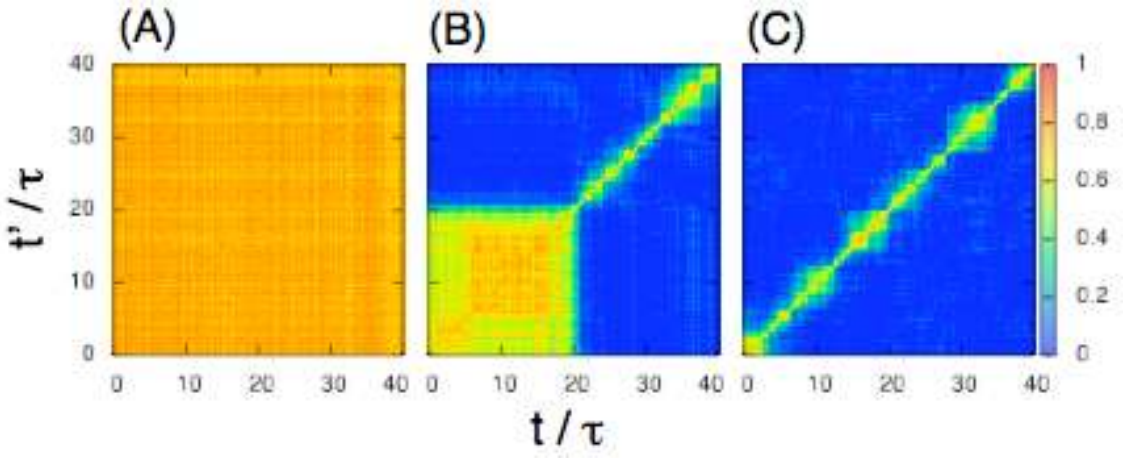

Fig. 4. Space-time interface at phase coexistence. Representative overlap matrices $Q(t,t') = N^{-1}\sum_{i=1}^{N}\cos\left\{\mathbf{q}\bullet\left[\mathbf{r}_i(t)-\mathbf{r}_i(t')\right]\right\}$, taken from the ensemble of trajectories at the coexistence field s^*, for $k_BT/\varepsilon = 0.6$, $t_{\text{obs}} = 40\tau$ and $N = 150$ (see Fig. 2Bb). (A) Typical trajectory from the inactive phase (from the low K_s peak in Fig. 2F), where for all observation times the correlation function remains close to 1, indicating non-ergodic dynamics. (B) Typical trajectory at coexistence (for values of K_s in the trough of Fig. 2F), where the overlap matrix shows a sharp interface-like structure at $t/\tau \approx 20$ separating an inactive region of space-time at earlier times, and an active region at later times. (C) Typical trajectory from the active phase (from the high K_s peak in Fig. 2F), where the system's dynamics is ergodic and the correlation function decays rapidly to zero. The inhomogeneous features evident in panel (C) are finite size effects which would vanish in the limit of infinite size, $N \to \infty$.

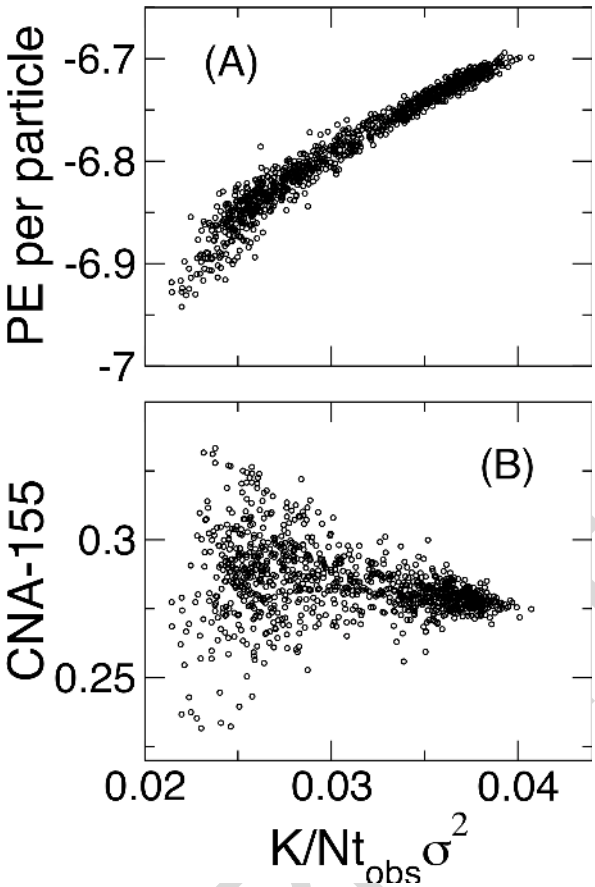

Fig. 5. Test of correlation between space-time order parameter and potential energy and icosahedral order. (A Potential energy per particle versus dynamical order-parameter K of a trajectory. (B) Icosahedral order, as quantified by the CNA-155 parameter of the common neighbor analysis, as a function of K. Results are for trajectories at $k_B T / \varepsilon = 0.6$, $t_{\text{obs}} = 40\,\tau$ and $N = 150$.